Materials Letters 148 (2015) 138–141

Contents lists available at ScienceDirect

Materials Letters

journal homepage: www.elsevier.com/locate/matlet

Using positive pressure to produce a sub-micron single-crystal column of cesium iodide (CsI) for scintillator formation

Chih Yuan Chen [a], Shih Hsun Chen [a], Chien Chon Chen [a,*], Jin Shyong Lin [b,**]

[a] Department of Energy Engineering, National United University, Miaoli 36003, Taiwan
[b] Department of Mechanical Engineering, National Chin-Yi University of Technology, Taichung 411, Taiwan

ARTICLE INFO

Article history:
Received 24 December 2014
Accepted 18 February 2015
Available online 25 February 2015

Keywords:
Material
Cesium iodide
Positive pressure
Ceramic
Single-crystal

ABSTRACT

The scintillator can be directly coupled to a commercial CCD and has the fastest response time (several ns) for real-time radiography. Most scintillator material production uses an expensive vacuum deposition process or a single-crystal growth method. This work reports the development of a cost-effective way to prepare sub-micron scintillator cesium iodide (CsI) columns in a ceramic anodic aluminum oxide (AAO) template by a positive pressure penetration method. Positive pressure can decrease the iodine vapor pressure and increase the CsI sublimation point up to the CsI melting point. Because the CsI melt is confined to an AAO channel with a high aspect ratio, the melt easily solidifies into a stable single-crystal CsI column. The SEM images showed CsI in a single crystal with a column diameter of 440 nm, smooth surfaces, and no grain boundaries. This positive pressure penetration method enables fabrication of a single-crystal CsI column with controllable size.

1. Introduction

Inorganic crystal scintillators have medium to high stopping power due to their high density and atomic numbers. The cesium iodide CsI scintillator material is commonly used in X- or γ-ray detectors. An X-ray detector using the CsI material is well suited to a computed tomography system [1,2]. CsI has a simple cubic structure, and the cations of Cs^+ are located at each of the corners of a cube, while the center of the cube is a single anion of I^-. The percent ionic (%IC) character of a bond between the elements Cs and I may be approximated by the expression [3], where X_I and X_{Cs} are the electronegativities for the I and Cs

$$\%IC = (1 - \exp[-(0.25)(X_I = X_{Cs})]) \times 100 \quad (1)$$

Because $X_I = 2.5$ and $X_{Cs} = 0.7$, the CsI compound includes 55.5% ionic bonding and partial covalence bonding. Due to the amount of ionic bonding in CsI, CsI can be dissolved in polarized H_2O to form CsI aqueous solution. CsI has a high solubility in water, and the solubility increases as temperature increases. For example, the solubility of CsI in H_2O ranges from 44 to 205 wt% at 10 and 90 °C, respectively [4].

Dendrites, bobbles, and grain boundaries form easily in an ionic compound when an uncontrolled melt solidifies. For example, a cesium iodide (CsI) melt easily forms three-dimensional defects on the free surface. The defects in the dendrites or bobbles in the grains form inside the CsI as the melt solidifies. Such defects can affect the X- or γ-ray path in the CsI crystal and decrease the scintillation characteristics.

In our previous research [5–7], we have made pure metals, alloys, and CsI columns by vacuum and mechanical injection methods. The SEM images showed each CsI column has smooth surface without any grain boundary of single crystal structure. The XRD pattern showed most of CsI columns in AAO template presented to (110) and (200) planes [8]. This work reports the development of a convenient low-cost approach to fabricating a CsI single crystal column using a positive pressure penetration procedure and an anodic aluminum oxide (AAO) template.

2. Experimental procedure

The procedure includes AAO fabrication. CsI nano-particles form on the AAO inner pore wall, and a CsI column forms inside the AAO channel. The following details describe the formation of AAO, CsI nano-particles, and a CsI column. The experimental chemicals including $HClO_4$, $CH_3(CH_2)_3OCH_2CH_2OH$, C_2H_6O, CrO_3, H_3PO_4, $CuCl_2$,HCl, and CsI bought from Merck Company in reagent grade.

* Corresponding author. Tel.: +886 37 382383; fax: +88637382391.
** Corresponding author. Tel.: +886 4 23924505x7174; fax: +886 4 23930681.
E-mail addresses: chentexas@gmail.com (C.C. Chen), linjsh@ncut.edu.tw (J.S. Lin).

http://dx.doi.org/10.1016/j.matlet.2015.02.089
0167-577X/

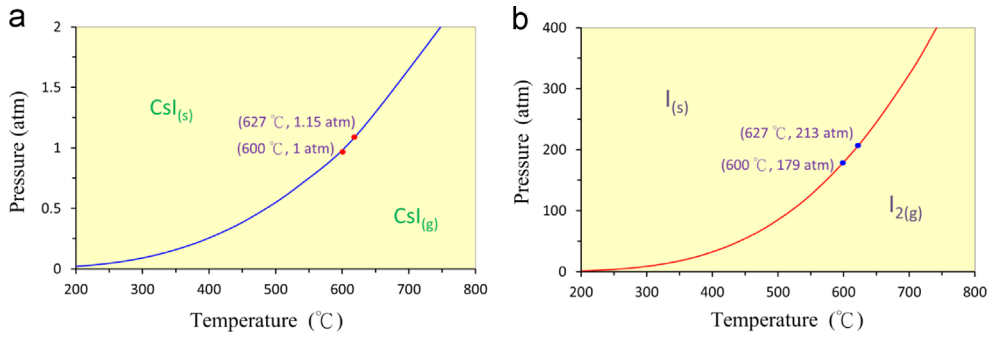

Fig. 1. The vapor pressures of CsI and I powders from 200 to 700 °C were calculated based on the Clausius Clapeyron Equation; (a) the $CsI_{(s)}$ sublimation vapor pressures are 1 atm and 1.15 atm at 600 °C and 627 °C, (b) the $I_{(s)}$ sublimation vapor pressures are 179 atm and 213 atm at 600 °C and 627 °C.

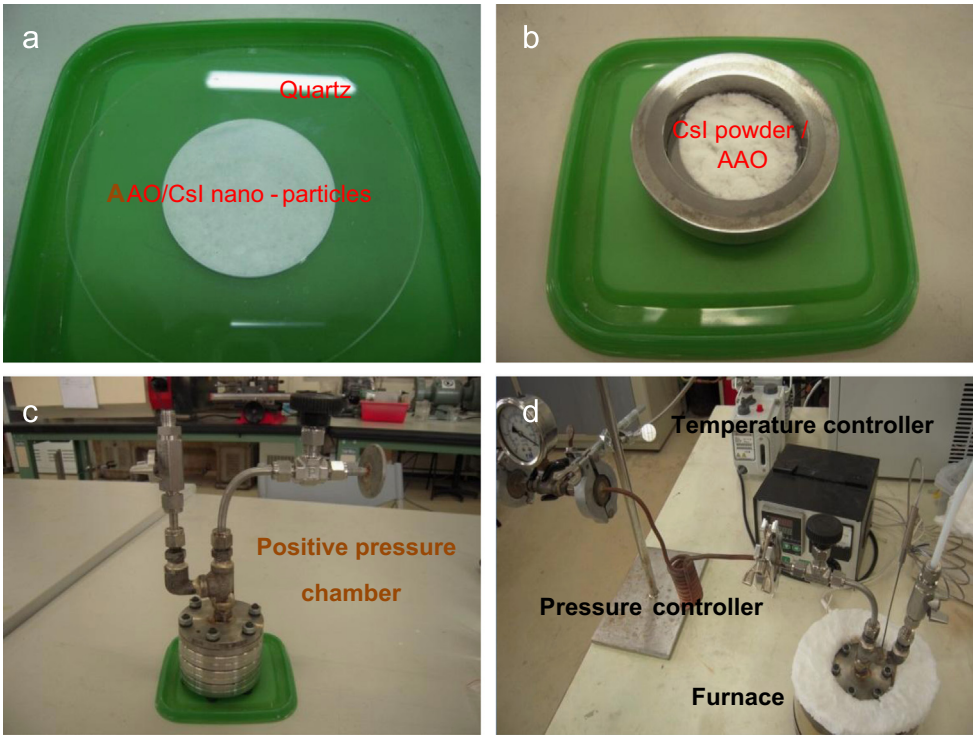

Fig. 2. The experimental setup for CsI column fabrication by CsI melt, AAO, and a high temperature positive pressure chamber; (a) AAO/CsI nano-particle template, (b) CsI powder on the AAO template, (c) AAO template/CsI powder in a positive chamber, and (d) heating CsI powder to the melting point.

AAO template: AAO film was made by anodization procedure, the steps including: (a) electrolytic polishing of Al substrate (15 vol % $HClO_4$ + 15 vol% $CH_3(CH_2)_3OCH_2CH_2OH$ + 70 vol% C_2H_6O, at 42 V), (b) 1st anodization (1 vol% H_3PO_4, at 200 V), (c) removal of 1st anodization film (1.8 wt% CrO_3 + 6 vol% H_3PO_4 + 92 vol% H_2O at 70 °C), (d) 2nd anodization (1 vol% H_3PO_4, at 200 V), (e) pore widening (5 vol% H_3PO_4, for 4 h), and (e) removal of Al substrate (8 wt% $CuCl_2$ + 5 vol% HCl + 85 vol% H_2O, for 3 min).

CsI nano-particles: In order to facilitate the CsI melt into the AAO template, CsI nano-particles were first formed on the AAO inner pore wall by wet deposition method (1 wt% CsI, at 25 °C for 3 min) and then the CsI nano-particles were sintered in an atmosphere furnace (400 °C for 5 min).

CsI column: The AAO sample with CsI nano-particles adhered and CsI powder on the surface was put on a quartz slice first, and then the AAO sample/quartz combination was placed inside a positive pressure chamber (10 atm Ar gas) and heated (650 °C for 1 min). Under these conditions, the CsI melt could flow into the AAO template. The microstructure and composition of the fabricated samples were studied using scanning electron microscope (SEM, JEOL 7400) and X-ray energy dispersive spectroscopy (EDS, Inca X-Stream).

3. Results and discussion

The sublimation, melting, and boiling points of cesium iodide compound are 600 °C, 627 °C, and 1277 °C under 1 atm, respectively. Therefore, the CsI vapor appears before the melting point. When the chamber pressure is less than 1 atm, the CsI has a lower sublimation point. The relationship between the sublimation point and pressure can be evaluated by the Clausius Clapeyron equation [9], where P, ΔH, T, R, and C are pressure (atm), enthalpy of vaporization (J/mole K), temperature (K), gas constant (8.314/J), and integration constant, respectively

$$\left(d\ln P = \frac{\Delta H}{RT^2}dT \quad or \quad \ln P = \frac{-\Delta H}{RT} + C\right) \tag{2}$$

Because CsI has vaporization enthalpy of 33,205 (J/mole K) [10] at 600 °C under 1 atm, the integration constant of CsI can be

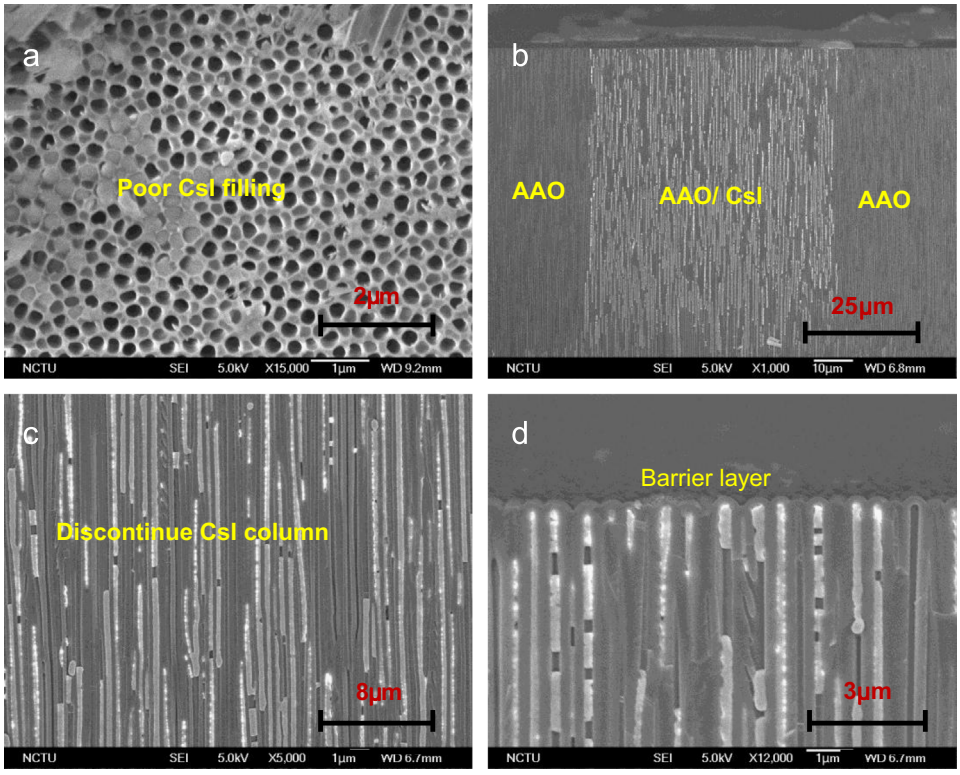

Fig. 3. SEM images of CsI columns with poor filling in AAO under 1 atm pressure at 650 °C; (a) top view of CsI partially filling the AAO template, (b) side view of CsI columns partially filling in AAO template, (c) side view of partial and discontinuous CsI columns in AAO, and (d) discontinuous CsI columns inside the AAO bottom.

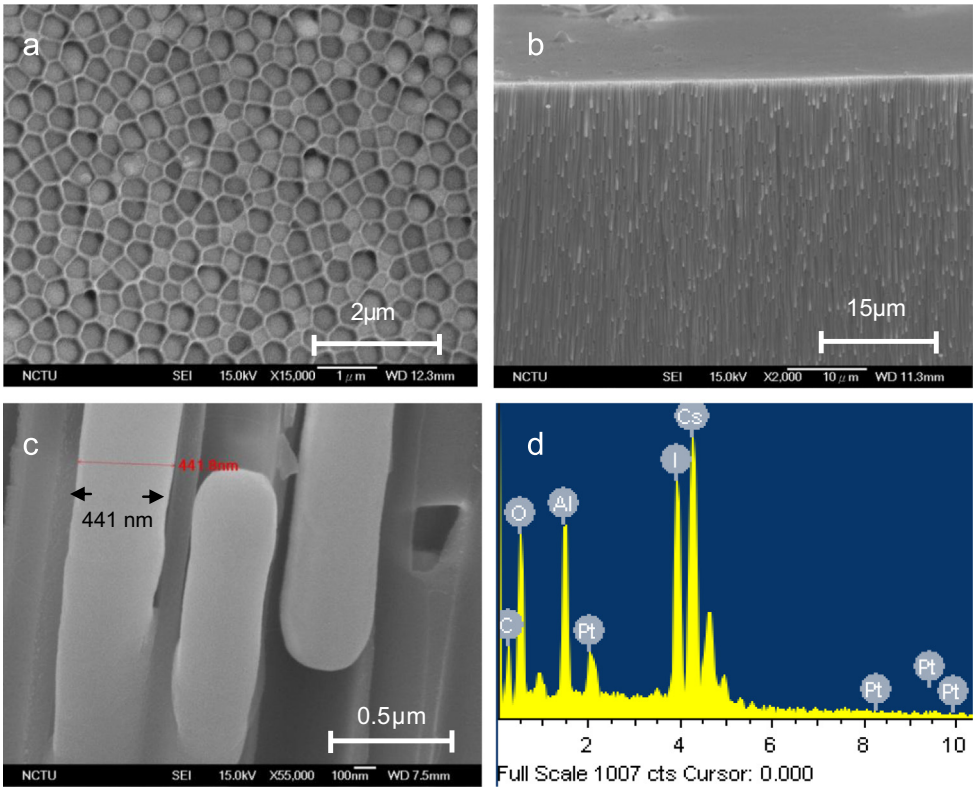

Fig. 4. SEM images of CsI columns with good filling of AAO template under 10 atm pressure at 650 °C; (a) top view of CsI filling AAO template, (b) side view of CsI columns inside AAO, (c) CsI column with diameter of 440 nm, and (d) EDS spectrum of CsI columns inside AAO.

calculated as 4.57, and the Clausius Clapeyron equation for CsI is expressed as

$$\ln P = \frac{-3993.9}{T} + 4.57 \quad (3)$$

According to this calculation, I has a vaporization enthalpy of 41,570 (J/mole K) [10] at 184 °C under 1 atm. The integration constant of I can be calculated as 10.94, and the Clausius Clapeyron equation for I is expressed as

$$\ln P = \frac{-41570.3}{T} + 10.94 \quad (4)$$

Based on Eqs. (3) and (4), Fig. 1 shows the vapor pressures of $CsI_{(g)}$ and $I_{(g)}$ from 200 to 700 °C. The $CsI_{(g)}$ vapor pressures are 1 atm and 1.15 atm (Fig. 1(a)) and the $I_{(g)}$ vapor pressures are 179 atm and 213 atm at 600 °C and 627 °C (Fig. 1(b)). The results in Fig. 1 shows that below 1 atm, the $CsI_{(g)}$ and $I_{(g)}$ vapors form below the $CsI_{(s)}$ melting point of 627 °C. Increasing the reaction chamber pressure can increase the CsI sublimation point up to the melting point and decrease the vapor pressure of $I_{(g)}$.

Fig. 2 shows the experimental setup of the CsI submicron column formation in the AAO template. (a) Using the pre-deposited CsI nanoparticles of AAO as a template, (b) the CsI powder is put on the AAO template, (c) the AAO template/CsI powder is placed in a positive chamber, and (d) the CsI powder is heated to the melting point and held for several minutes. The CsI melt can then permeate into the AAO channels and solidify as submicron CsI columns. It is interesting that when the CsI melt is confined to an AAO channel, it grows as a stable single wire without any dendrites, consistent with previous theoretical predictions [7].

We also compared the quality and microstructure of CsI columns that formed under pressures of 1 atm and 10 atm. Fig. 3 shows SEM images of CsI columns that formed on the AAO template under 1 atm pressure at 650 °C. As we discussed above, when the CsI/AAO sample was under a lower pressure at high temperature, large amounts of $CsI_{(g)}$, $I_{2(g)}$, and $CsO_{x(g)}$ vapors were produced on and in the AAO, so not enough CsI melted on the AAO surface, leading to discontinuous CsI columns inside the AAO template. Fig. 3(a) shows a top view image of the CsI/AAO sample with a low quality of CsI filling in the AAO template, and Fig. 3(b) shows a side view image of CsI columns only partially filling the AAO template. Fig. 3(c) shows a side view image of partial and discontinuous CsI columns in the AAO template. Fig. 3(d) shows that the CsI melt was able to penetrate to the bottom of the AAO template, but the CsI columns were discontinuous.

According to the curves in Fig. 1, $CsI_{(s)}$ has a sublimation point of 1450 °C, which is higher than its melting point of 627 °C at 10 atm pressure. Pure $I_{(s)}$ has a sublimation point of 308 °C. However, the $I_{2(g)}$ from CsI compound has a sublimation point higher than 308 °C under 10 atm. Fig. 4 shows SEM images of CsI columns with good filling of the AAO template, produced under pressure of 10 atm at 650 °C. The higher pressure in the chamber prevented the vapors from forming in the chamber. In detail, Fig. 4(a) is a top view image of CsI filling the AAO template; Fig. 4(b), a side view image of CsI columns inside AAO; Fig. 4(c), CsI with a column diameter of 440 nm and a smooth surface, with no grain boundary, indicating it is a single crystal CsI column; and Fig. 4(d), an EDS spectrum indicating Cs, I, Al, and O in the CsI columns inside the AAO template.

4. Conclusions

This novel and simple method offers a cost-effective approach to the fabrication of high-value CsI columns. A CsI melt can penetrate into AAO channels of various sizes and solidify into CsI nano-wire or sub-micron CsI columns. Because the CsI column can produce greater quantities of photo-electrons than CsI nano-wire for the scintillator use described in this paper, we chose to use a pore size of 450 nm on the AAO template to produce sub-micron CsI columns. The positive pressure limits the formation of CsI and $I_{2(g)}$ vapors before the melting point of CsI is reached, allowing the production of a high quality CsI column.

Acknowledgments

This work was financially supported by the Chung-Shan Institute of Science and Technology (CSIST) under the Contract no. CSIST-442-V103 and, National Science Council, Taiwan under the Contract no. 103-2221-E-239-004.

References

[1] Stampanoni M, Borchert G, Wyss P, Abela R, Patterson B, Hunt S, et al. Nucl Instrum Methods Phys Res A 2002;491:291–301.
[2] Ananenko A, Fedorov A, Lebedinsky A, Mateychenko P, Tarasov V, Vidaj Y. Quantum Electron Optoelectron 2004;7:297–300.
[3] Callister WD. Materials science and engineering. USA: Mc Graw Hill; 1994. p. 28.
[4] ⟨http://en.wikipedia.org/wiki/Solubility_tableC⟩.
[5] Chen CC, Bisrat Y, Luo ZP, Schaak RE, Chao CG, Lagoudas DC. Nanotechnology 2006;17:367–74.
[6] Chen SH, Chen CC, Luo ZP, Chao CG. Mater Lett 2009;63:1165–8.
[7] Chen CC, Fang D, Luo ZP. Rev Nanosci Nanotechnol 2012;1:229–56.
[8] Chen CC, Chang SF, Luo ZP. Mater Lett 2013;112:190–3.
[9] Rao YK. Stoichiometry and thermodynamics of metallurgical processes. ISSBN:0 521 25856 1. USA; 1985 p 526.
[10] Chase MW, Davies Jr. CA, Downey JR, Furip Jr. DJ, McDonald RA, Syverud AN. JANAF thermochemical tables. 3rd ed. New York, USA: American Chemical Society; 1985. p. 95960.